Photoenhanced metastable deep trapping in amorphous chalcogenides near room temperature

M. Abkowitz and R. C. Enck
Xerox Corporation, 800 Phillips Road, Webster, New York 14580
(Received 4 October 1982; revised manuscript received 31 January 1983)

Deep trapping of injected holes or electrons is temporarily enhanced at room temperature in chalcogenide films which have undergone prior near-band-gap photoexcitation at room temperature. Persistence of this effect can be measured by xerographic techniques which are very sensitive to relatively small changes in trapped-space-charge density. Xerographic techniques can also be used to monitor and compare the release rates of carriers trapped in photosensitized and dark-rested samples. Measurements have been made on glasses in the As:Se:Te system but the present results are restricted to *a*-Se, which is ambipolar. There are four principal results: (1) Distinct decay times for the persistence of photoenhanced metastable hole and electron deep trapping are observed. Metastable electron traps decay away more slowly than their hole counterparts. (2) Photosensitization of deep trapping in *a*-Se is a bulk effect which exhibits a characteristic wavelength and exposure dependence. (3) In both dark-rested and photoexcited samples, average release time of trapped electrons is larger than average release times of trapped holes. (4) ESR is not observed in either the photoexcited or dark-rested samples at room temperature. Results are discussed phenomenologically and in terms of a specific low-energy point-defect model proposed for chalcogenides.

INTRODUCTION

Reversible thermal and light-induced changes in amorphous semiconductor microstructure have been under active investigation for some time. Particular interest is aroused when observations suggest that these microstructural changes effect optical and electrical behavior. Examples of such light-induced phenomena are the photodarkening and photovolumetric effects in chalcogenides[1] and the Staebler-Wronski effect in *a*-Si.[2] A principal example of a thermally induced effect is the observation of hysteresis behavior in many of the photoelectronic properties (drift mobilities, lifetime, generation efficiences) of chalcogenides during thermal cycling[3–6] (i.e., fixed-rate heating and cooling in the vicinity of T_g). Analysis of optical and electrical measurements can in turn be used to relate thermal or light-induced microstructural changes to specific changes in the electronic density of gap states.

Standard techniques for studying deep gap electronic structure like thermally stimulated currents (TSC), field effect, and photoconductivity have recently been augmented by the application to amorphous systems of space-charge spectroscopies,[7] initially developed to study crystalline semiconductors in device configuration. Deep-level transient capacitance and photocapacitance and bias-dependent junction capacitance are well-known examples. Classified among these space-charge spectroscopies should be equally powerful, but less (generally) familiar xerographic techniques[8,9] developed to characterize electrophotographic photoreceptors. Recently, one such technique, the time-resolved measurement of xerographic residual potential[9] has been used to map the electronic density of deep gap states in *a*-Se. In this paper, xerographic residual measurements are used to study the effect of prior photoexcitation history on the range of injected carriers in amorphous Se films. Data will be presented for *a*-Se only but similar effects are observed (at room temperature) on alloy films throughout the Se:As:Te system. It will be demonstrated that both the injected-hole and injected-electron range are reduced (i.e., deep trapping is increased) significantly in *a*-Se films which have undergone prior photoexcitation with near-band-gap light. This photoenhanced trapping is metastable, decaying away as the specimen film dark rests (i.e., the electroded film is typically rested in the dark under short-circuit conditions at 295 K). The nominal relaxation time is about an hour at room temperature, but is in fact different for the electron- and hole-metastable traps.

In the following, exposure and spectral depen-

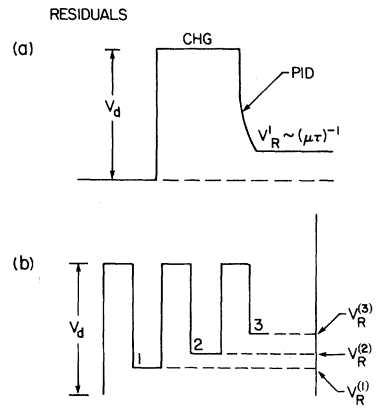

FIG. 1. (a) Schematic voltage profile of a sample during a single xerographic cycle. V_d is the voltage to which the sample is charged. After photoinduced discharge (PID), the residual potential is inversely proportional to the injected carrier $\mu\tau$ product. (b) Repeated xerographic cycling causes the residual to buildup ("cycle-up").

dence of photosensitized metastable deep trapping are first described. Spatial distribution of trapped charges after xerographic cycling is compared in dark-rested and in photosensitized samples. The respective relaxation functions of electron- and hole-metastable trapping (lifetimes of the metastable centers) are determined at room temperature. The respective distributions of trap release times (distribution of trap depths) in dark-rested and bulk photoexcited films are then compared. Finally, observations are discussed in general phenomenological terms, then examined with respect to defect models.[10,11]

BACKGROUND

Figure 1(a) is the voltage profile of a film during a single xerographic cycle. The cycle is initiated by a charging step (corona or transient contact to a power supply). The sample film of capacitance C is charged to a voltage V_d of either polarity. During photoinduced discharge (PID) by strongly absorbed light some fraction of the transiting charge (i.e., fraction of CV) falls into deep traps, and the resulting trapped space charge is manifested as a residual potential V_R. Residual potential will be either positive or negative depending on charging polarity. With repeated cycling the residual (i.e., residual potential) builds up as shown in Fig. 1(b). The residual potential, measured using a capacitively coupled electrometer, can be related to the space-charge distribution function. A one-dimensional formulation is appropriate,

$$V_R=\epsilon_0^{-1}\epsilon^{-1}\int_0^L dx\int_0^x \rho(x')dx' , \tag{1}$$

where L is the sample thickness, ϵ is the relative dielectric constant, ϵ_0 the free-space permitivity, and $\rho(x)$ the space-charge density. For the case of uniform bulk space-charge density ρ_0, the above simplifies,

$$V_R=\rho_0 L^2/2\epsilon_0\epsilon,\quad \rho_0=Ne , \tag{2}$$

where N is the number of electronic charges, e, per unit volume. Notice that as few as 10^{12} electronic charges per cm^3 in a 50-μm selenium film ($\epsilon=6.4$) give rise to a 4-V residual which is easily measured. It is readily shown that use of the spatially uniform trapping approximation to estimate the number of trapped charges from the residual potential introduces serious error (i.e., error factor of 10) only when the trapped space-charge distribution is sharply skewed towards the substrate. Skewing of trapped space charge toward the free surface of the film, for example, introduces an error factor of no more than 2.

The key experimental parameter characterizing deep trapping is the $\mu\tau$ product. If μ is taken to be the drift mobility, then τ is the real-time lifetime measured in a time-of-flight experiment. $\mu\tau$ is directly related to the trapping parameters N and $\langle\sigma\rangle$:

$$\mu\tau=\mu_0/(N\langle\sigma\rangle v_{\rm th}) , \tag{3}$$

where N is the number of traps per cm^3 and $\langle\sigma\rangle$ their average cross section. μ_0 is the microscopic mobility, and $v_{\rm th}$ the carrier thermal velocity. The product $\mu\tau$ can be determined directly from the first-cycle residual potential of a well-rested sample of thickness L. According to Kanazawa and Batra,[12] in the weak-trapping limit, when $V_R \ll V_d$ (V_d is the charging voltage),

$$V_R/V_d=(0.5L^2/\mu\tau V_d)[-\ln(2V_R/V_d)] . \tag{4}$$

In the strong-trapping limit ($V_R \sim V_d$), these authors derive the corresponding relationship

$$V_R/V_d=1-(\mu\tau V_d/L^2)(\ln 2). \tag{5}$$

In general, where comparisons have been made, $\mu\tau$ computed from the xerographic residual potential using these expressions agrees well with results of drift mobility experiments on the same specimen.

Under repeated xerographic cycling, the residual builds to a saturation value. When cycling ceases the residual potential decays as the space charge equilibrium is reestablished. Analysis of a set of residual curves parametric in temperature enables the distribution of trap energies to be determined.[8,9]

EXPERIMENTAL

a-Se films 55 μm thick were prepared by vacuum evaporation at a rate of 2 μm/min onto oxidized aluminium substrates held at 55 °C, which is about 18 °C above the glass transition temperature. The aluminium-oxide blocking layer which formed the substrate interface was approximately 50 Å thick.

Xerographic measurements were carried out either in the corona or electroded mode. In the corona mode, xerographic measurements were made on a reciprocating sample stage. The sample was first passed under a corona charging device, the corotron, which could be set to deposit either positive or negatives ions on the sample surface (the corona contact is blocking). The charging circuitry ensured that a fixed quantity of charge was delivered to the samples per cycle independent of their surface voltages. After charging, the sample was moved to a measuring station where surface voltage could be determined using a transparent capacitively coupled electrometer probe. The time from termination of the charging step to the onset of surface voltage measurement was a few tenths of a second. Either the dark decay or the photoinduced discharge characteristic (PIDC) following step or flash illumination with strongly absorbed light could be measured.[13] Small-signal time of flight could also be measured for both carriers in the xerographic mode[14] [xerographic time of flight (XTOF)]. In the latter case, the transit of a small packet of charge, photoexcited at the top surface by a weak, 4-nsec pulse of strongly absorbed light could be resolved in the electrostatic field established by prior corona charging. In the present study, time of flight normally used to elucidate transport behavior was principally used to probe the internal field distribution[14,15] (from which the space-charge distribution is determined) as it changed during repeated xerographic cycling. In the electroded mode[9] samples were provided with semitransparent top contacts. In this case charging was by transient contact to a dc power supply with the entire sequence controlled by tandem pulse-delay generators or a microprocessor. In the electroded mode the sample is motionless during the entire cycle sequence. The response time limitation is thus set by the sample circuit and electrometer. Xerographic cycle parameters can also be varied over an extremely wide range.

The photoexcitation history of typical sample specimens was as follows. The sample was first preilluminated for a specified time under zero-field conditions with either filtered or white light. Tungsten halogen light (3300 K) was filtered using dielectric interference filters with a bandpass of 10 nm full width at half maximum. White-light illumination from the same source was filtered to pass between 400—800 nm. White-light photon flux was experimentally determined using a detector whose quantum efficiency versus wavelength was accurately known. A blackbody spectral characteristic was assumed for the 3300-K source. After light exposure the sample was allowed to rest in the dark under zero-field conditions for a rest time τ which was varied. After rest the sample was typically cycled once. Erasure of the surface charge was by exposure to strongly absorbed light. The residual potential and the residual decay immediately following exposure were measured. In some experiments cycling was repeated and the cycle up[9,13] and residual decay characteristics were also recorded. In the present study the temperature was fixed at about 294 K. ESR experiments were carried out in an X-band spectrometer at room temperature. Sensitivity was about 10^{12} spins/G. Typical power level was about one milliwatt.

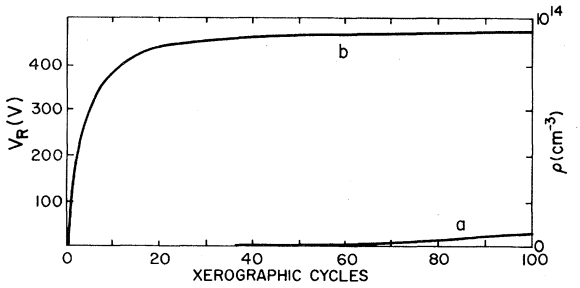

FIG. 2. Residual voltage versus number of xerographic cycles in a 55-μm a-Se film at $T=295$ K. Curve a: dark-rested film. Curve b: film irradiated for 15 min in a white-light flux of 2×10^{15} photon/cm^2 sec. Cycling begins after 1 min dark rest. Equivalent space charge density represented by right ordinate scale.

RESULTS

In Fig. 2, we compare the buildup of positive residual potential in a 55-μm thick a-Se film after prolonged dark rest (curve a) and after only a 1 min dark rest following a 15-min white-light exposure ($F=2\times10^{15}$ photons/cm^2 sec) (curve b). The figure illustrates the principal results of the present study. It is found that the residual potential measured after a single xereographic cycle, the rate of residual buildup during repeated cycling (cycle-up), and the saturation residual (value approached after prolonged cycling) are all enhanced in samples exposed to white light prior to measurement. For example, the figure shows that the positive residual after 100 cycles is enhanced more than an order of magnitude in the irradiated film. A similar effect is observed for the negative xerographic residual potential.

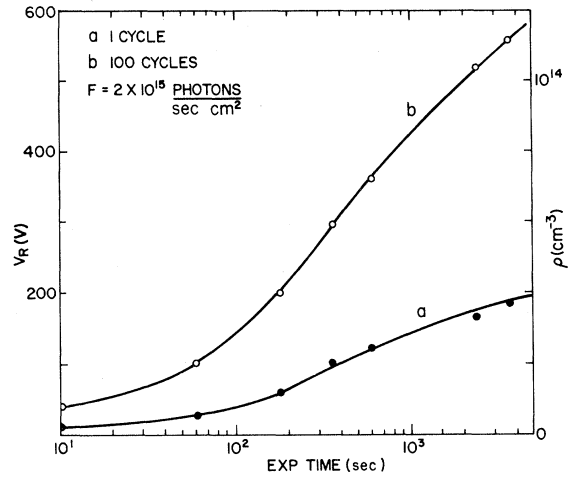

FIG. 3. Residual voltage in a 55-μm a-Se sample after (a) one xerographic cycle and (b) after 100 xerographic cycles vs exposure time. Sample is subjected to a white-light flux of 2×10^{15} photons/sec cm^2 for the exposure time, then dark rested 1 min prior to cycling.

The photoenhancement of injected carrier deep trapping depends on exposure. Figure 3 illustrates this exposure dependence of the sample to broadband light. The effect of exposure on the first cycle residual (a) is compared to the corresponding effect after completion of one hundred cycles (b). Exposure dependence is observed for a wide range of exposure times. For very short exposure, residuals approach those measured on the dark-rested specimen. For very long exposures the enhanced trapping effect tends to saturate.

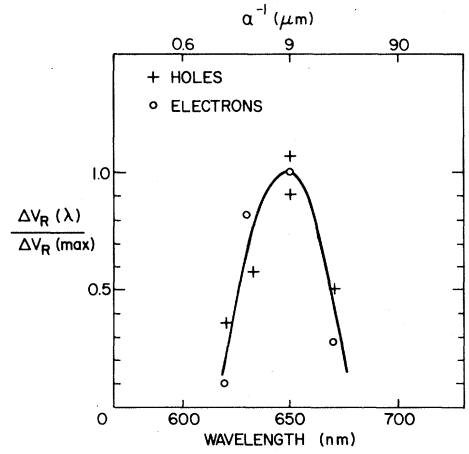

FIG. 4. Relative enhancement of first-cycle positive (+) and negative (circles) residual after fixed exposure at the wavelengths indicated. Sample is 55-μm a-Se, $T=295$ K, $\Delta V_R(\lambda)$ is the increase above dark-rested residual after exposure. ΔV_R (max) occurs near 650 nm.

At fixed exposure photosensitization of deep trapping is wavelength dependent. Figure 4 shows the relative enhancement of positive and negative first-cycle residual versus excitation wavelength produced by fixed exposure to monochromatic light. Strong wavelength dependence was observed between 600—700 nm. This wavelength dependence was the same for electron and hole trapping with maximum sensitization occurring near 650 nm. At 650 nm, absorption depth is about 9 μm. Optimum sensitization clearly occurs when radiation penetrates the bulk. Monochromatic sensitizing radiation was produced by filtering white light through three-cavity dielectric interference filters having 10 nm full width at half maximum. The drop off at long wavelengths can probably be attributed to a combination of factors. The specimen becomes increasingly transparent as wavelength is increased, while the generation rate of free carriers per absorbed photon progressively diminishes. Drop off at short wavelengths can probably be attributed to some surface specific property such as enhanced carrier recombination.[16] Alternatively, a natural limit to the sensitization can ensue as the exciting radiation is absorbed in a progressively decreasing volume.

The spatial distribution of bulk trapped charge is determined from analysis of xerographic time-of-flight (XTOF) measurements. In the XTOF experiment a sheet of carriers photoexcited at the sample film's top surface drifts across the bulk under the combined action of the uniform field established by prior corona charging and the local field produced by any trapped space charge. In the present study all transit pulses observed in the space-charge free sample are rectangular with a Gaussian tail. Pulse shapes exhibit a characteristic distortion[14,15] when there is trapped homocharge. The information contained in the pulse shape which is a display of the derivative of the surface voltage versus time, is equivalent, in the small signal limit, to current versus time in a conventional electroded time-of-flight (TOF) measurement. If the drift mobility is independent of position, then the magnitude of the XTOF waveform at any time is proportional to the local electric field at the instantaneous position of the drifting charge centroid. The transformation from the derivative of surface voltage versus time to internal local electric field versus position is carried out by recognizing that the instantaneous position of the charge sheet is proportional to the photoinduced voltage change at that time (equal to the time integral up to that time of the XTOF waveform). The spatial derivative of the local electric field gives the space-charge distribution from Poisson's equation.

Employing this procedure the space-charge distribution after 100 xerographic cycles was determined

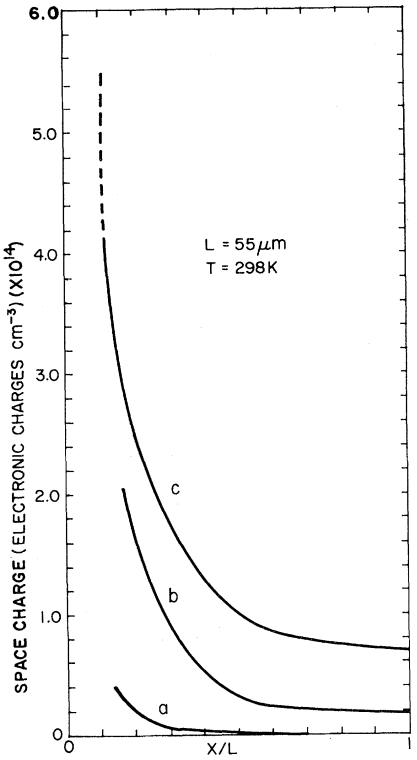

FIG. 5. Positive space charge profile in an $L=55$ μm a-Se sample, $T=298$ K, after 100 xerographic cycles. Sample was subjected to white irradiation at a flux $F=2\times10^{15}$ photon/sec cm^2 of duration a, 10 sec; b, 10 min; c, 60 min. Light incident on top surface at $X=0$. Sample was dark rested 1 min prior to cycling.

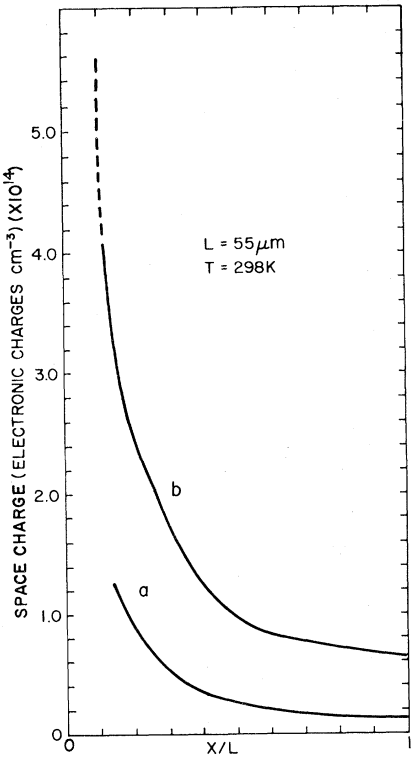

FIG. 6. Positive space charge profile developed in a 55-μm a-Se sample at $T=298$ K after (a) a single xerographic cycle, (b) 100 xerographic cycles. Prior to cycling sample had been exposed for 60 min to a white-light flux of 2×10^{15} photons/cm^2 sec, then dark rested 1 min.

following white-light irradiation of varying duration. Data are displayed in Fig. 5. Exposure was to a white-light flux of 2×10^{15} photons/sec cm^2 for a, 10 sec; b, 10 min; c, 60 min. Light was incident on the top ($x=0$) surface. The calculated profile is fully consistent with the distribution of absorbed photons for white-light illumination and, in addition, reflects the exposure dependence already illustrated in Fig. 3. The corresponding residual voltages are a, 40 V; b, 360 V; c, 560 V. Figure 6 displays the respective space-charge profiles induced by a single xerographic cycle (a) and 100 xerographic cycles (b) following 60 min of exposure to a white-light flux of 2×10^{15} photons/cm^2 sec. In the measurement used to obtain Figs. 5 and 6, the sample was dark rested one minute after irradiation, prior to xerographic cycling.

The persistance of light-sensitized deep trapping can be represented by a relaxation function. The experimental relaxation function is determined as follows: the specimen is subjected to a fixed exposure, then allowed to dark rest for a time τ which is experimentally varied. After time τ residual voltage $V_R(\tau)$ is measured after completion of a single xerographic cycle. The relaxation function is then defined as

$$[V_R(\tau)-V_R(\infty)]/[V_R(0)-V_R(\infty)]\ . \tag{6}$$

$V_R(0)$ is the first-cycle residual voltage measured immediately after termination of irradiation. $V_R(\infty)$ is the residual in a completely dark-rested sample.

Figure 7 compares relaxation functions for the light-induced metastable trapping of (a) holes and (b) electrons in an a-Se sample at $T=297$ K. There is a significant difference in persistence of the effect for holes and electrons. In neither case can the decay be characterized by a single relaxation time. There was some sample-to-sample variability noted for the hole metastable trapping relaxation function. However, in all cases persistence of the effect for

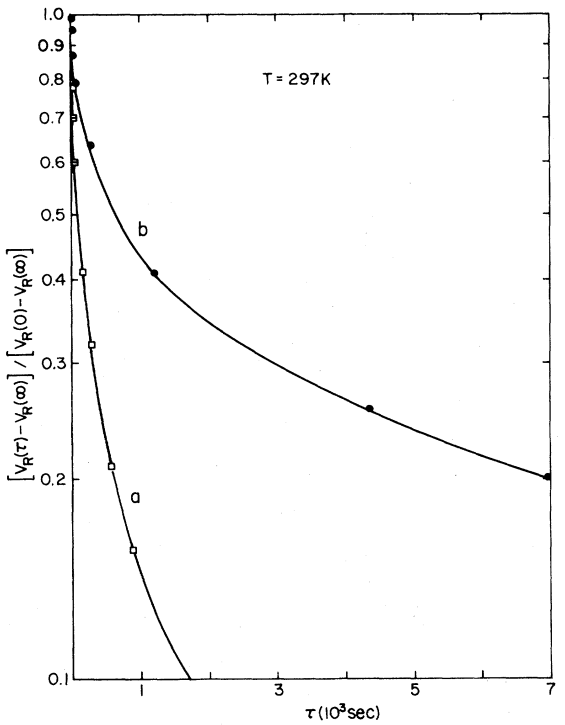

FIG. 7. *a*-Se relaxation plot (see text) for (*a*) hole-trapping metastables and (*b*) electron-trapping metastables. τ is the dark-resting time after irradiation is terminated. $T=297$ K, $L=55$ μm. White-light irradiation was 5 min in a flux of 2×10^{15} photon/sec cm^2.

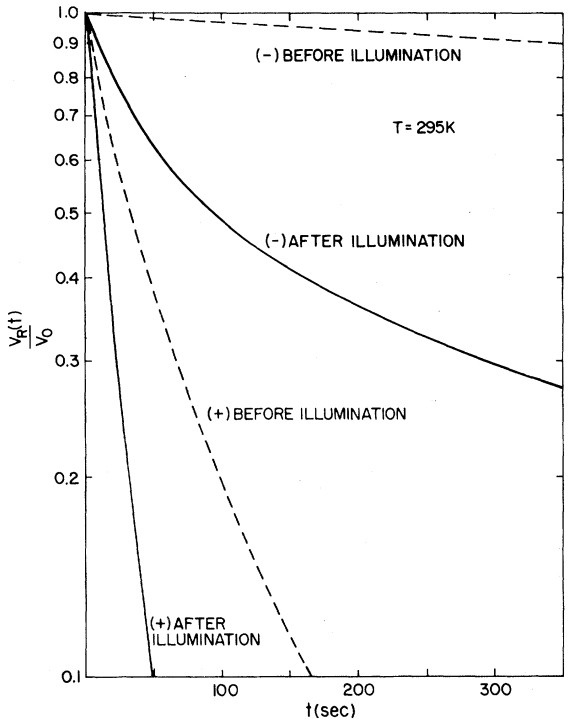

FIG. 8. Semilogarithm plot of positive and negative normalized residual potentials vs time $T=295$ K, $L=55$ μm. Dashed curves are for dark-rested specimen. Solid curves for specimen subjected to a white-light flux of 2×10^{15} photons/sec cm^2 and dark rested 1 min prior to single xerographic cycle.

electrons significantly exceeded that for holes as illustrated.

The relaxation function describes the persistence of light-sensitized deep trapping. In other words, how long the metastable centers themselves live (i.e., metastable trap lifetime). It is also possible to independently measure their energy distribution (i.e., the distribution of metastable trap release times). The latter is accomplished by time resolving the isothermal decay of residual potential created by charge injected into traps during xerographic cycling after bulk photoexcitation.[9] Typical room-temperature data is displayed in Fig. 8. Residual decay data, which is displayed on a logarithmic scale, is normalized to the $t=0$ residual value (i.e., residual immediately after the final xerographic photodischarge). Dashed curves labeled ($-$) and ($+$) are the respective decay curves for electrons and holes in a sample which had been dark rested prior to measurement. The solid curves were obtained on samples with the following illumination history. The sample was subjected to a five minute white-light irradiation in a flux of 2×10^{15} photon/sec cm^2. The sample was then dark rested 90 sec and subjected to a single xerographic cycle. The time-varying residual voltages after photodischarge were recorded and plotted on a normalized logarithmic scale as indicated. The residual potential decay functions reflect the distribution of underlying trap release times. Qualitative comparison of solid and dashed curves shows that trap distributions become skewed toward shallower energies for both electrons and holes in irradiated samples.

It is interesting that xerographic cycling experiments demonstrate that capture of a photoinjected carrier onto a sensitized site does not immediately restore the precursor state. If the sensitized sample is cycled to saturation, then allowed to undergo complete residual decay it will, if recycled immediately, continue to show enhanced trapping of the photoinjected carriers. The latter is consistent with the observation that the metastable trap lifetimes are larger than the metastable trap release times.

Finally the effect of preillumination on states controlling the drift mobility of injected carriers was determined using the XTOF technique described earlier. Typical results are illustrated in Fig. 9. XTOF hole transients are shown for a 55-μm *a*-Se

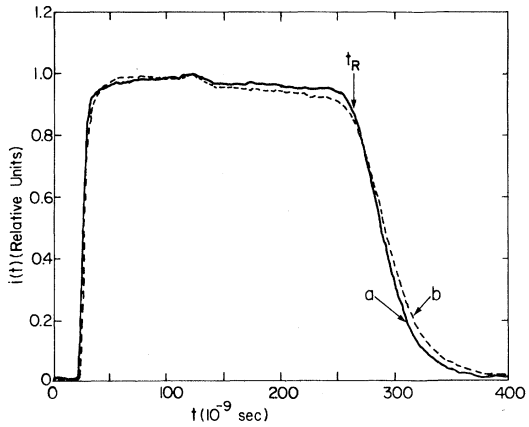

FIG. 9. XTOF hole transients for a 55-μm Se sample after dark rest, curve *a*, and after 5-min white-light exposure (2×10^{15} photons/sec cm^2), curve *b*. Transients were taken after corona charging to + 730 V. The transit time indicated on the figure, t_R, is essentially identical for the two sample treatments.

film after dark rest, curve *a*, and then after a 5-min white-light exposure ($F=2\times10^{15}$ photons/sec cm^2), curve *b*. Transients were taken after corona charging to +730 V. The principal result is highlighted by the vertical arrow on the figure. The transit time t_R is identical in *a* and *b*. Preillumination was found to have no effect on electron or hole transit times.

DISCUSSION

Deep trapping of injected electrons and holes is comparably enhanced at room temperature in samples preexposed to penetrating light at room temperature. Such preillumination can cause an order-of-magnitude increase in the deeply trapped (positive or negative) space-charge density induced by xerographic cycling, but has no corresponding effect on drift mobility of either sign carrier. Drift mobility in *a*-Se is controlled by shallow traps. Enhanced deep trapping is dependent on exposure, an effect manifested over a wide range of exposure times and on spectral composition of the exciting light. Geometrical distribution of trapped charge after white-light sensitization is consistent with the optical absorption profile of white light in the specimen. All observations support the conclusion that photosensitized deep trapping is a bulk effect. Lifetimes of the sensitized hole and electron trapping effects were measured, and electron metastable trapping was found to persist longer than the analogous hole trapping. The relative energy distribution of sensitized centers were measured by analyzing residual potential decay.

In the following, results are first discussed phenomenologically. Phenomenological arguments appear to place specific requirements on the trap states involved. These requirements are compared to the behavior predicted if metastable traps derive from chalcogen bonding miscoordination defects.[10,11]

We consider first two alternative phenomenological interpretations of light enhanced trapping.

(1) Light alters occupancy of a fixed preexisting population of localized electron states. The usual picture is that normally empty precursor states (i.e., states that exist in equilibrium before the solid is photoexicted) became filled during preillumination. As a result of the nonequilibrium occupation of electronic gap states, physical properties (i.e., optical, dielectric, and electrical) are altered. Thermal processes then reestablish equilibrium occupancy restoring properties characteristic of the dark-rested solid. The latter is the mechanism suggested to explain other, more commonly observed, light-induced metastabilities in amorphous films such as fatigue[13] and persistent conductivity. Fatigue and persistent conductivity[13] occur when traps (normally empty states) become filled and are thereby temporarily converted to recombination or thermal emission centers (in the simplest one-electron model of a one-carrier system, the photoexcitation which produces fatigue and persistent conductivity simultaneously reduces the number of traps).

Preillumination affects not only the rate of development of trapped space charge during the xerograhic cycling of *a*-Se ("residual cycle up"[9]), but also the saturation residual potential which measures the maximum number of trapped charges the specimen can accommodate. Since the absolute number of traps is assumed to be invariant, photoenhanced space-charge buildup must be a result of an increase in the average cross section of deep traps. In fact, prolonged (bulk) irradiation (zero applied field) enhances the number of experimentally visible traps by about an order of magnitude ($\sim10^{15}$ cm^{-3}) with respect to the dark-rested sample. The model therefore requires at least 10^{15} cm^{-3} traps whose cross sections are small enough to render them invisible during conventional xerographic cycling experiments on dark-rested specimens. These states are thus clearly distinct from the 10^{14} cm^{-3} traps normally made visible by xerographic experiments on unsensitized *a*-Se films.[9]

To reiterate, if we chose to assume that the total number of gap states is fixed, the experimental observations force us to the additional conclusion that most of these states are invisible as traps until the specimen is photosensitized.

(2) Light creates new electronic gap states. Rever-

sible and irreversible optical and structural changes have been observed in various chalcogenide glasses including *a*-Se.[1] One set of phenomena is observed at temperatures below 100 K.[1,17] Another distinctive set of phenomena is observed near room temperature.[1] In certain cases experimental results suggest that light can create localized defect electronic states.[18,19] There is no evidence, apart from that presented in the present study, to suggest that any of the reported photoinduced optical and structural changes effect the transport of charge in chalcogenides. (Thermally induced structural transformations, on the other hand, significantly affect electrical behavior of chalcogenides.[3,4,6,8])

At temperatures below 40 K, band-gap photoexcitation produces luminescence, photoinduced absorption, and photoparamagnetism in chalcogenides.[17] Changes in the thermodynamic behavior of glassy specimens below 1 K have also been induced by excitation with band-edge light, presumably by elminating states which act as tunneling centers.[20] All of this behavior was originally interpreted solely in terms of light-induced transient repopulation of preexisting localized electronic gap states.[17] More recent studies,[18,19] however, indicate that prolonged low-temperature irradiation of chalcogenides can in fact create defect electronic states near midgap in direct association with reversible photostructural changes. In both the original studies of Bishop, Strom, and Taylor,[17] and in the work of Biegelson and Street[19] on photodefect creation, photoparamagnetism and induced absorption could be eliminated by subband-gap irradiation or by annealing to 150 K. Significant memory effects were observed when low-temperature photoexcitation was repeated immediately after 150 K annealing.[19] The latter suggesting two simultaneous but distinct photoeffects, namely (1) defect creation and (2) the trapping of photoexcited carriers at defects transforming these to paramagnetic centers. All of these low-temperature effects including the memory effect are completely removed by warming the specimen to room temperature.

Low-temperature experiments demonstrate that light can create defect electronic states. Tanaka[1] has reported extensively on both reversible and irreversible room-temperature photodarkening and photovolumetric effects. However these room-temperature effects have not been identified with localized defect electronic states near midgap. Tanaka's experiments, in fact, provide no direct evidence for such states. These room-temperature effects have instead been identified with changes in the degree of quantitative disorder in the glassy network.[1] On the other hand, xerographic experiments may be providing the first evidence that deep defects can also be created by room-temperature irradiation. In the following, experimental results are therefore reexamined in terms of specific point defect models[10,11] proposed for chalcogenides.

COMPARISON WITH THE CHARGED DEFECT MODEL

To simultaneously rationalize key optical, magnetic, and electronic properties of amorphous chalcogenides, it has been proposed that alternately charged native defects always exist in some quasiequilibrium population.[10,11] It has been further proposed that these alternately charged defect pairs are typically a positive threefold-coordinated and a negative onefold-coordinated chalcogen atom.[11] The electronic configuration of these defects is spin paired and is made energetically favorable by strong electron-phonon coupling which leads to a negative effective correlation energy.[21] These defects are produced in pairs at little cost in energy and exist in equal concentrations in the melt if no other charged species (chemical) are introduced.[22] It is proposed that defect pair production is initiated by rupture of a chalcogen atom bond. The resulting dangling bond is a high-energy defect which interacts with the nonbonding *p* electrons (lone pair electrons) of a neighboring chalcogen atom to produce the alternately charged lower-energy defect pair.[11] It has been suggested that these defects can exist as bound pairs [intimate valance alternation pairs (IVAPS)] or in disassociated form (VAPS). The defect pair model is predicated on a negative effective correlation energy. If the correlation energy is instead positive the lowest-energy defect becomes a dangling bond which is neutral and paramagnetic.

The buildup and decay of low-temperature luminescence and photoparamagnetism in chalcogenides have been interpreted in terms of such native defect states.[9] Photodefect creation at low temperature has also been interpreted in terms of native defects. Qualitatively identical photoactive behavior is observed in important chalcogen binary systems containing Ge and Se and As and Se, respectively, and in pure amorphous selenium itself. (Luminescence efficiency is smaller and photoparamagnetism weaker[23] in *a*-Se.) The low-temperature experimental data has been interpreted as being consistent with the existence of charged defect pairs (IVAPS or VAPS), which have a diamagnetic ground state. These exist in equilibrium in the melt and are frozen in during glass formation. Their number is presumably enhanced at low temperature by prolonged (damage producing) irradiation.[19] It has been proposed that photoexcited neutral paramagnetic species can be generated by a set of identical transi-

tions from both the native and photogenerated defect pairs.[19]

Comparison of the present results on room-temperature photoenhanced metastable trapping with the low-temperature data,[17–19,23] and with the native defect models just described prompts the following comments.

(1) The integrated number of deep traps observed after prolong irradiation of *a*-Se at room temperature by xerographic techniques is many orders of magnitude smaller than the number of paramagnetic centers[18,19] excited by comparably low-temperature irradiation.

(2) ESR is not observed in dark-rested *a*-Se films.[24] Neither were we able to detect any room-temperature paramagnetism after room-temperature irradiation sufficient to produce about 10^{15} cm^{-3} (xerographically detected) electron- and hole-metastable deep traps in *a*-Se. (It should be noted that the effective ESR sensitivity for any magnetically anisotropic system can be significantly reduced by *g*-factor broadening in the glassy state.)

(3) From (1) and (2) we conclude that the present experiments provide no clear evidence that photoenhanced deep trapping at room temperature is specifically related to low-temperature photoluminescence and photoparamagnetism.

(4) If light creates no new states than for reasons described earlier there must be a mechanism capable of greatly enhancing the trapping cross sections (for both signs of the injected carrier) of (what are initially) very-small cross-section traps. The conversion of neutral traps to attractive Coulombic centers by the capture of photoexcited carriers seems perhaps most physically plausible. The latter would imply however that the preponderant near-midgap defect states are a population ($\sim 10^{15}$ cm^{-3}) of neutral species distinct from the traps which control space-charge buildup during xerographic cycling of the dark-rested film. In this regard it is interesting that recent calculations of Vanderbilt and Joannopoulos[25] suggest a positive correlation energy for *a*-Se leading to the prediction that a neutral dangling bond would be the lowest-energy native defect. The neutral dangling bond should however be paramagnetic and ESR is not observed in the dark-rested film.[24]

(5) In the absence of fully definitive evidence the explanation of photoenhanced deep trapping based on photodefect creation remains appealing. In this picture breaking a bond could lead either to formation of a defect pair or a dangling bond depending on the sign of the correlation energy. The problem is that (a comparable population of) hole- and electron-metastable traps are observed to decay at different rates in the dark which appears to rule out (for the case of negative correlation energy) direct recombination of alternately charged defect pairs. On the other hand, if the lowest-energy defects are (neutral) dangling bonds, two distinct neutral species appear to be required.

To sustain the charged—defect-pair picture (negative correlation energy) operationally requires the existence of an intermediate buffer state. This buffer would temporarily store the excess charge released by the more rapidly deactivated hole-metastable trap. The buffer state must be present at a concentration considerably exceeding that of the traps observed xerographically in the dark-rested sample. Furthermore, the buffer cannot act as a trap for injected charge. Given these constraints we suggest that the buffer would most likely be a decay intermediate of the hole-metastable trap itself.

SUMMARY AND CONCLUSIONS

(1) Deep trapping of injected holes or electrons is temporarily enhanced in *a*-Se (and in Se-rich alloys in the As:Se:Te system) after near-bandgap photoexcitation. For example, a 60-min exposure of a 55-μm *a*-Se film to a white-light flux of 2×10^{15} photons/cm^2 sec increases the deep trapping of both carriers about an order of magnitude. Photosensitization of deep trapping is a bulk effect which exhibits characteristic wavelength and exposure dependence.

(2) After bulk photoexcitation ceases, distinct decay times for the persistence of metastable hole and electron deep trapping are observed. Electron trapping metastables decay more slowly than their hole counterparts.

(3) In both dark-rested and photoexcited samples the average release times of trapped electrons is larger than the average release times of trapped holes.

(4) ESR is not observed in either the photoexcited or dark-rested samples at room temperature.

(5) Two alternative phenomenological explanations have been suggested. The first is that capture of bulk photoexcited electrons and holes by very small cross-section precursor states converts them to larger cross-section traps. The second is that light creates point defects by breaking bonds. The former requires that a large number of neutral low cross-section defects exist near midgap in the dark-rested film. The latter needs to be reconciled with the observation that hole and electron metastable traps decay at different rates in the dark.

[1]For an overview, see K. Tanaka, in *Fundamental Physics of Amorphous Semiconductors,* Proceedings of the Kyoto Summer Institute, Kyoto, Japan, 1980, edited by F. Yonezawa (Springer, New York, 1981), p. 104. Also see K. Tanaka, in *Proceedings of the 7th International Conference on Amorphous and Liquid Semiconductors,* edited by W. E. Spear (University of Edinburgh Press, Edinburgh, 1977) p. 787.

[2]D. L. Staebler and C. R. Wronski, J. Appl. Phys. 51, 3262 (1980).

[3]M. Abkowitz and D. M. Pai, Phys. Rev. B 18, 1741 (1978).

[4]M. Abkowitz and R. C. Enck, in *Proceedings of the Eighth International Conference on Amorphous and Liquid Semiconductors, Cambridge, Massachusetts, 1979,* edited by W. Paul and M. Kastner (North-Holland, New York, 1980), p. 831. Also as J. Non-Cryst. Solids 35-36, 831 (1980).

[5]M. Abkowitz, in *The Physics of Selenium and Tellurium,* Vol. 13 of *Springer Series in Solid State Sciences,* edited by E. Gerlach and P. Grosse (Springer, Berlin, 1979), p. 210.

[6]M. Abkowitz Ann. N. Y. Acad. Sci. 371, 170 (1981).

[7]D. V. Lang, in *Thermally Stimulated Relaxation in Solids,* Vol. 37 of *Springer Series Topics in Applied Physics,* edited by P. Braunlich (Springer, Berlin, 1979), p. 93.

[8]M. Abkowitz and R. C. Enck, in Proceedings of the Ninth International Conference on Amorphous and Liquid Semiconductors, Grenoble, France, 1981, edited by B. K. Chakraverty and D. Kaplan [J. Phys. (Paris) Colloq. 42, C4-443 (1981)].

[9]M. Abkowitz and R. C. Enck, Phys. Rev. B 25, 2567 (1982).

[10]N. F. Mott, E. A. Davis, and R. A. Street, Philos. Mag 32, 961 (1975).

[11]M. Kastner, D. Adler, and H. Frtitzsche, Phys. Rev. Lett. 37, 1504 (1976).

[12]K. K. Kanazawa and I. P. Batra, J. Appl. Phys. 43, 1845 (1972).

[13]M. Schaffert, *Electrophotography* (Focal, New York, 1975).

[14]S. B. Berger, R. C. Enck, and G. M. T. Foley, *Proceedings of 1980 International Symposium on Industrial Uses of Selenium and Tellurium, Toronto, Canada* (Selenium Tellurium Development Association Inc., Darien, Ct., 1980), p. 179.

[15]M. Scharfe and M. D. Tabak, J. Appl. Phys. 40, 3230 (1969).

[16]D. M. Pai and R. C. Enck, Phys. Rev. B 11, 5163 (1975); R. C. Enck and G. Pfister, in *Photoconductivity and Related Phenomena,* edited by J. Mort and D. M. Pai (Elsvier, Amsterdam, 1976), Chap. 7, p. 215.

[17]S. G. Bishop, A. Strom, and P. C. Taylor, Phys. Rev. Lett. 34, 1346 (1975); Phys. Rev. B 15, 2278 (1977) and references therein.

[18]F. Mollot, J. Cernogora, and C. Benoît a la Guillaume, in *Proceedings of the Eighth International Conference on Amorphous and Liquid Semiconductors, Cambridge, Mass., 1979,* edited by W. Paul and M. Kastner (North-Holland, New York, 1980), p. 939.

[19]D. K. Biegelsen and R. A. Street, Phys. Rev. Lett. 44, 803 (1980).

[20]D. L. Fox, Brage Golding, and W. H. Haemmerle, Phys. Rev. Lett. 49, 1356 (1982).

[21]P. W. Anderson, Phys. Rev. Lett. 34, 953 (1975).

[22]N. F. Mott, Philos. Mag. 34, 1101 (1976).

[23]S. G. Bishop, U. Strom, E. J. Friebele, and P. C. Taylor, J. Non-Cryst. Solids 32, 359 (1979).

[24]M. Abkowitz, J. Chem. Phys. 46, 4537 (1967).

[25]D. Vanderbilt and J. D. Joannopoulos (unpublished).